Internal structure of an ex-vessel corium debris bed during severe accidents of LWRs

Eunho Kim [a], Jin Ho Park [a], Kiyofumi Moriyama [a], Hyun Sun Park [a*]
[a]*Division of Advanced Nuclear Engineering(DANE), Pohang university of science and technology (POSTECH), 77 Chuongam-Ro, Nam-gu, Pohang, Gyungbuk, Republic of KOREA, 790-784*
[*]*Corresponding author: hejsunny@postech.ac.kr*

1. Introduction

Severe accidents of light water reactors (LWRs) involve significant melting of the core fuel. The hot molten core fuel can threaten the integrity of the boundaries of defense-in-depth (DID) barriers for preventing the release of radioactive materials to public and environment. The coolability of ex-vessel corium directly affects the integrity of the containment building and determines the likelihood of termination or mitigation of accidents.

In the wet cavity strategy, the deep coolant pool with moderate melt release rate allows the corium to break up into small debris particles and make porous debris beds on the bottom of the water pool in reactor cavity. For conducting an exact coolability assessment and devising a reasonable accident management plan, it is required to understand the nature of the debris bed. In the aspect of the coolability assessment the configuration of the debris bed, including internal and external characteristics, has significant importance as boundary conditions for simulations, however, relatively little investigation of the sedimentation process.

For the development of a debris bed, recently there have been several studies that focused on thermal characteristics of corium particles. Yakush *et al.* [1] performed simulation studies and showed that two-phase natural convection affects the particle settling trajectory and changes the final arrival location of particles to result more flattened bed. Those simulation results have been supported by the experimental studies of Kim *et al.* [2] using simulant particles and air bubble injection. For the internal structure of a debris bed, there have been several simulation and experimental studies, which investigated the effect of internal structure on debris bed coolability [3, 4]. Magallon has reported the particle size distribution at three elevations of the debris bed of FARO L-31 case, where the mean particle size was bigger for the lower elevation [5]. However, there is a lack of detailed information on the characteristics of the debris bed, including the local structure and porosity.

In this study, we investigated the internal structure of the debris bed using a mixture of stainless steel particles and air bubble injection. Local particle sedimentation quantity, particle size distribution change in radial direction and axial direction, and bed porosity was measured to investigate a relationship between the internal structure and the accident condition.

2. Experiment

2.1 Experimental facility

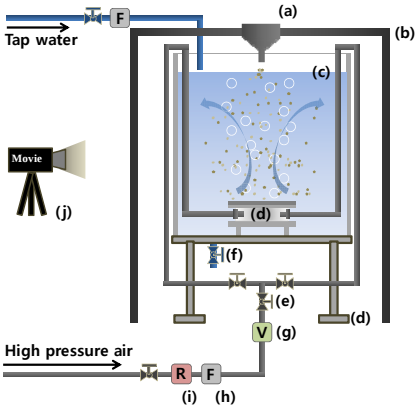

Fig. 1. A schematic diagram of the DAVINCI test facility: (a) funnel, (b) funnel rack, (c) test pool, (d) particle catcher plate module, (e) total flowrate controller, (f) water drain valve, (g) digital flow sensor, (h) mist separator, (i) pressure regulator, (j) digital cameras, "F" means a filter, "R" means a regulator, "V" means a volume flow meter

Figure 1 shows a schematic diagram of the DAVINCI (Debris Bed Research Apparatus for Validation of the Bubble-Induced Natural Convection Effect Issue) test facility in POSTECH, which was designed to simulate particle sedimentation in a flooded cavity. It is composed of a particle injection system, a test pool, and a particle catcher plate. The particle injection system is physically separated from the test pool to isolate the particle feeding from the vibration of convection flow in the pool. A funnel with an inner diameter of 23.5 mm was used to inject particles, and the particles were released by gravity by lifting a rubber plug in the nozzle. The test pool is made of a transparent acrylic cylinder, which is 1.0 m high with an internal diameter of 0.58 m, and the walls are 0.01 m thick. Filtered tap water was used in all experiments. The particle free-fall distance from the nozzle exit to the free surface of the pool was 75 mm, and the distance from the free surface to the particle catcher plate was 0.76 m. The particle release rate was ~ 0.35 kg/s.

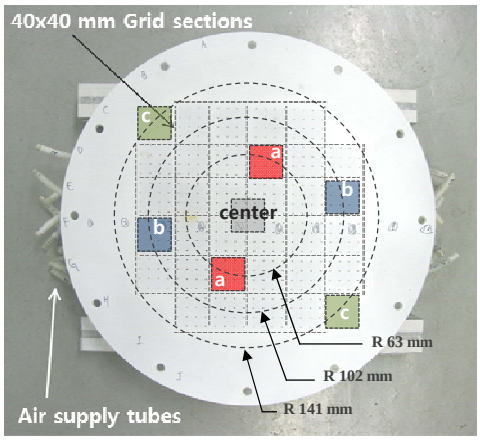

Fig. 2. A photograph of the particle catcher plate module and the location of particle sampling cups

Figure 2 shows the particle catcher plate module which is placed at the bottom of the test pool. It is composed with a catcher plate and air chambers. The catcher plate has a grid of 40 mm × 40 mm squares on the top. Each square in the grid has sixteen air bubble holes with a diameter of 1.5 mm, which are connected to an air chamber beneath the catcher plate. Vapor generation from the hot corium debris bed was simulated using air bubble injection for each of the grid sections with thirty-two air chambers in a pre-determined airflow rate distribution. Purified high-pressure air was used in all experiments.

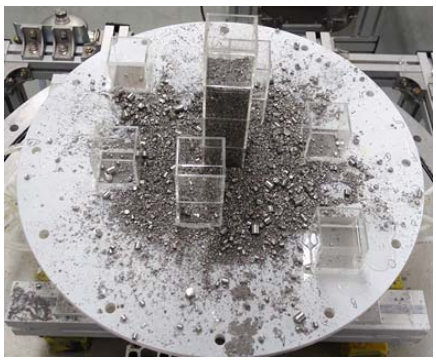

Fig. 3. A photograph of the particle sampling cups on the particle catcher plate module

Figure 3 shows particle sampling cups on the particle catcher plate module. The particle sampling cup is made of rectangular acrylic pipe unit; it is 40 mm high with an internal cross-section of 36 mm × 36 mm, and the walls are 2 mm thick. Total seven cups were placed in pre-determined positions; region a, b, c, and center (see **Fig. 2**). The region a is 63 mm away from the center in the radial direction, and the region b and c is 102 and 141 mm away, respectively. A stainless steel mesh with an aperture of 0.1 mm is placed on the bottom of the catcher cup to collect the settled particles while allowing air bubble penetration.

2.2 Simulant particles

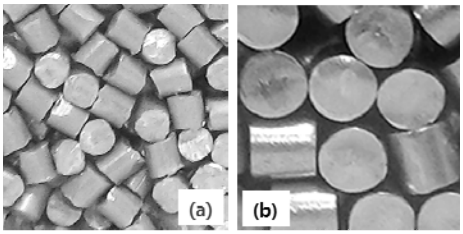

Fig. 4. A photograph of the simulant particles: (a) cut wire particle of 2.3 mm diameter, (b) cylindrical bearing roller particle of 6 mm diameter

Figure 4 shows the simulant particles, which are short cylinders. For a diameter of 0.2 ~ 2.3 mm, cut wire particles were used. For the simulant particles with a diameter of 4.0 ~ 8.0 mm, the cylindrical bearing rollers were used. Stainless steel 304 was used as the simulant material because of its high density (~ 8,000 kg/m^3), which is similar to that of the corium.

Table 1: Particle size distribution of test condition

D_v^* (mm)	Diameter (mm)	Mass Frac.	Mass (g)
0.23	0.2	2.3%	46.0
0.46	0.4	2.6%	51.6
0.69	0.6	4.8%	95.0
1.03	0.9	4.5%	89.9
1.37	1.2	6.8%	135.5
1.95	1.7	12.1%	241.8
2.63	2.3	19.1%	381.6
4.58	4.0	27.4%	547.6
6.87	6.0	13.3%	265.6
9.16	8.0	7.3%	145.5
sum		100.0%	2,000

*D_v (Equivalent Volume Sphere Diameter)

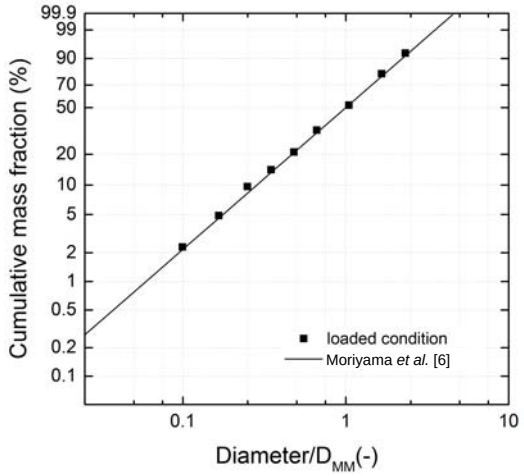

Fig. 5. The particle size distribution of test condition in cumulative mass fraction

Table 1 lists ten kinds of particles in different sizes, which were used to make a test particle mixture. Total 2 kg of the particle mixture was prepared for all test cases. The composition of particles in the test condition was

designed to simulate that of corium debris particles from breakup and fragmentation of the melt jet, by using the particle size distribution model of Moriyama *et al*. [6]. **Figure 5** shows a particle size distribution of the test condition of particle mixture with the empirical correlation of Moriyama *et al*. [6].

2.3 Test matrix

Table 2: Test cases and the total air injection rate (L/min)

	Case 1	Case 2	Case 3
Quiescent pool condition (QPC)	0	0	0
Two-Phase condition (TPC)	70.6	69.8	68.6

Table 2 lists two groups of test conditions used here. One was under quiescent pool conditions (QPCs) without bubble generation, and the other was under two-phase flow condition (TPCs) with bubble-induced two-phase natural convection flow. The QPC tests provided a reference situation. For TPC condition, about 70 lpm of air was injected in a center weighted manner. **Figure 6** shows the air injection rate distribution for each grid section on the particle catcher plate. Both conditions were conducted three times.

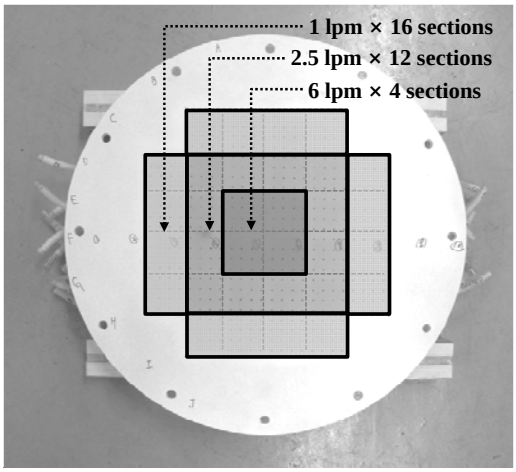

Fig. 6. Volumetric air injection rate of each grid section of the particle catcher plate module

2.4 Measurement

For measuring the particle size distribution of the resultant particle bed in axial and radial directions, we sampled particles from the particle sampling cups using a spoon with a sharp tip and a tweezer. The sampled particles were separated by size using standard test sieves, and weighed with an electronic scale (EK-4100i, AND), which has measuring uncertainty of ± 0.05g. Sampling in the axial direction was carried out for every 30 mm height.

2.5 Repeatability

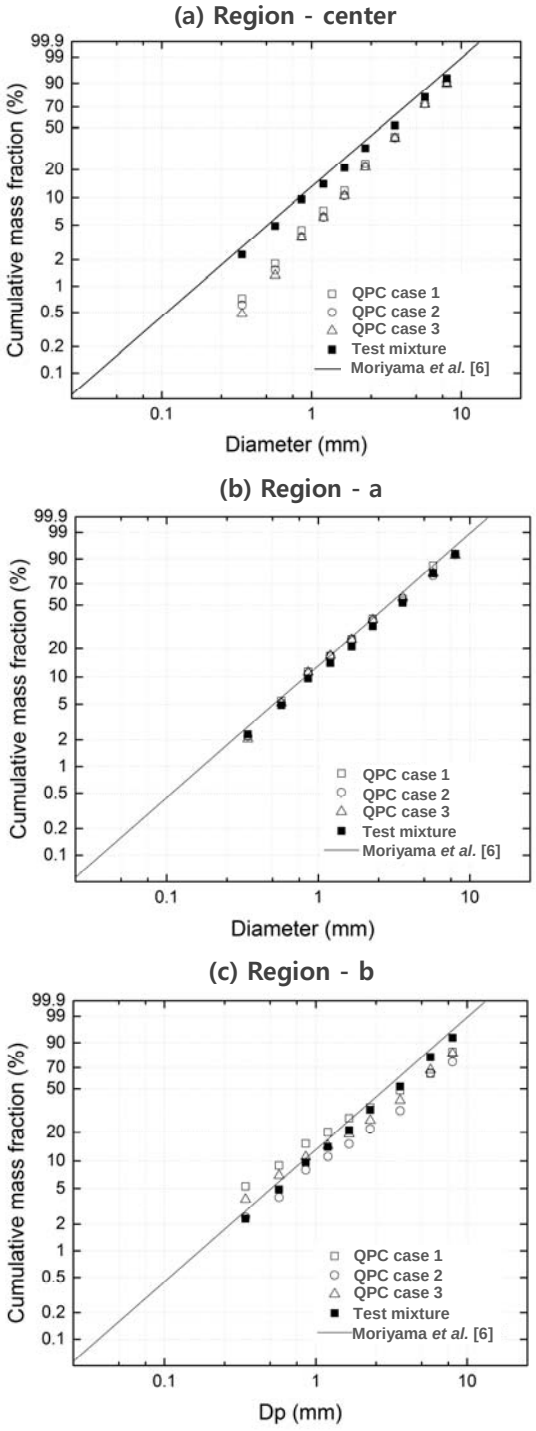

Fig. 6. Local particle size distribution of the quiescent pool condition (QPC): (a) center region, (b) region a, (c) region b

Figure 6 shows the local particle size distribution of three test cases of QPC including the center region, the region ‘a’, and the region ‘b’. The region ‘c’ was omitted, since there was too small sedimentation quantity to compare results.

Table 3 lists the average and standard deviation of the mass fraction of each particle size. The maximum

standard deviation of the center region was 0.57% for the size of 9.16 mm. In the region 'a' and region 'b', the maximum standard deviation were 4.52 % for 9.16 mm and 8.70% for 4.58 mm, respectively.

Table 3: Average and standard deviation of mass fraction [%]

D_v (mm)	Center region		Region a		Region b	
	Ave.	Std.	Ave.	Std.	Ave.	Std.
0.23	0.61	0.12	2.14	0.08	3.81	1.44
0.46	0.94	0.12	3.12	0.14	2.83	1.09
0.69	2.33	0.21	5.90	0.17	4.79	1.32
1.03	2.61	0.22	5.62	0.23	3.80	0.82
1.37	4.48	0.18	7.86	0.19	5.33	1.79
1.95	10.91	0.21	13.01	0.67	6.91	0.50
2.63	19.23	0.20	17.78	1.51	12.80	1.77
4.58	31.51	0.56	25.42	3.82	25.46	8.70
6.87	17.49	0.24	13.93	1.36	14.79	4.56
9.16	9.88	0.57	5.22	4.52	19.49	4.55

3. Results

3.1 Local particle sedimentation

Figure 7 shows the top views of the particle catcher plate after particle sedimentation of TPC and QPC. In the QPC tests, most of the particles fell directly in a narrow cylindrical column to make a center-symmetric sedimentation, and a small fraction of particles was scattered laterally due to hydraulic drag resistance and particle collisions. In the TPC tests, the sedimentation of particles exhibited rather one-sided and widespread manner due to the disturbance by the upward two-phase flow which distort the falling trajectories of particles.

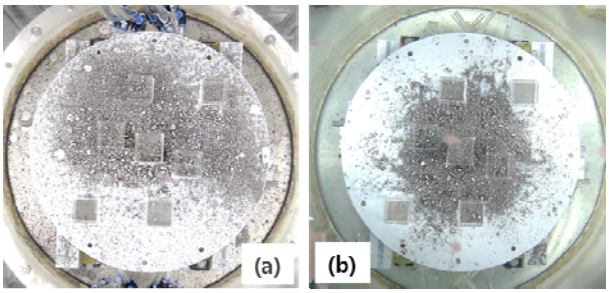

Fig. 7. Photographs of the particle catcher plate after tests: (a) case 2 of TPC, (b) case 2 of QPC

Figure 8 shows the total particle sedimentation quantity of the four local regions of the QPC and TPC tests. In the QPC tests, the particle sedimentation is highly concentrated on the center region, and it decreases rapidly with the radial distance from the center. In the TPC tests, at the center region, a much smaller proportion of the particles accumulated. For the region a, b, and c, the TPC tests were classified separately by heavy sedimentation side and light sedimentation side. The heavy sedimentation side has much more particles than both the light sedimentation side and the QPC tests. The light sedimentation side has less or similar particle quantity than the QPC tests.

It shows that two-phase natural convection induced by vapor generation from the corium debris bed strongly affects particle settling trajectories and also results in a more flattened particle bed.

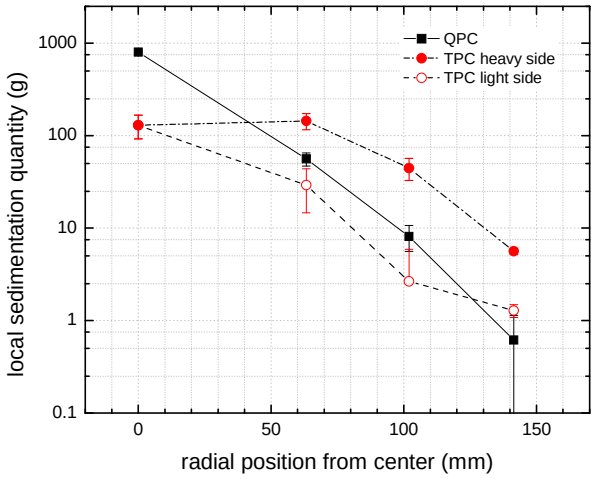

Fig. 8. The total particle sedimentation quantity for radial positions

3.2 Particle size distribution in radial position

Figure 9 shows the local particle size distribution of the tests of QPC and TPC for the four sampling regions including the region a, b, c, and the center region. The regions with less than 5 g of total sedimentation quantity were excluded: the light sedimentation side of the TPC tests in the region b and c, and the QPC tests in the region c.

Figure 9 (a) shows the particle size distribution at the center region. For both the QPC and TPC tests, the mass fraction of particles with small diameters decreased, while that of particles with large diameters increased. The degree of change was larger for the TPC tests than the QPC tests. **Figure 9 (b)** shows the particle size distribution at the region a, which is 63 mm away from the center of the particle catcher plate. While the QPC tests exhibited mostly similar size distribution to the test mixture, in the TPC tests, the mass fraction of particles with small diameters decreased and that with large diameters increased for both the heavy and light sedimentation sides. **Figure 9 (c)** shows about the region b, which is 102 mm away from the center. The heavy sedimentation side of the TPC tests exhibited mostly similar size distribution to the test mixture. In the QPC tests, the mass fraction of particles between the size of 1.03~4.58 mm decreased and the biggest particle size of 9.16 mm increased. **Figure 9 (d)** shows about the region c, which is 141 mm away from the center. The heavy sedimentation side of the TPC tests generally exhibited the increase of mass fraction of the small particles.

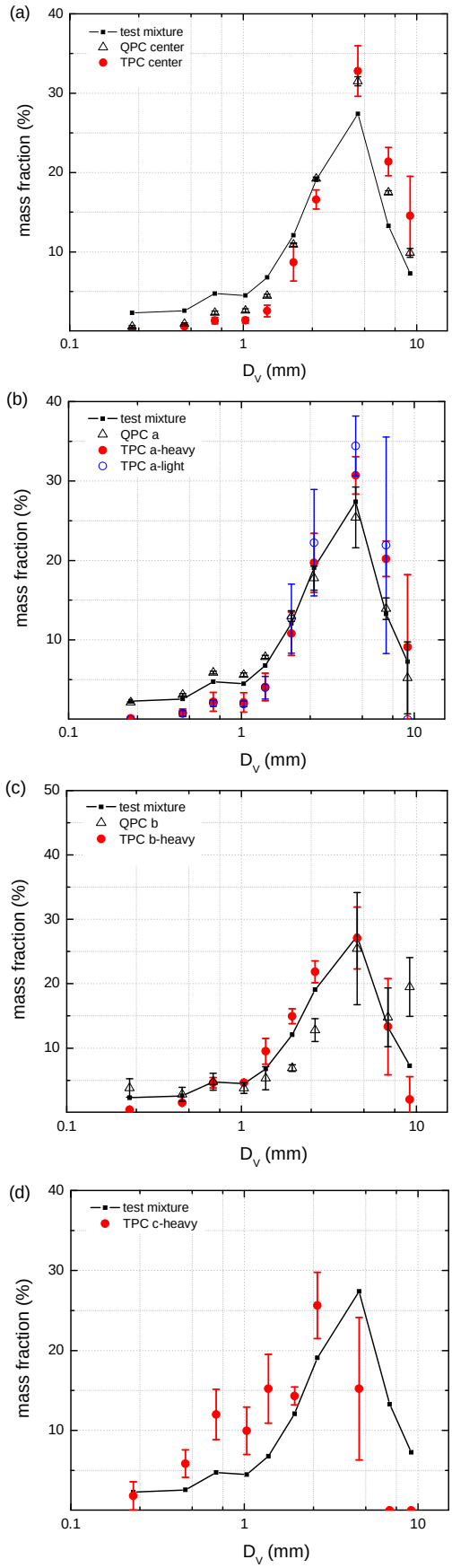

Fig. 9. Local particle size distribution for four regions: (a) center region, (b) region a, (c) region b, and (d) region c.

Based on the experimental results described above, the TPC tests showed that the particle size distribution changes to less sedimentation of smaller particles around the center and increase of mass fraction with radial distance. The QPC tests did not exhibit a clear trend of change, and the degree of change was also smaller than the TPC tests. In the TPC tests, there were not only the hydraulic drag resistance but also the countercurrent turbulent flow resistance by two-phase natural convection, which was induced by air injection rate of 70 lpm. More tests are necessary to understand the effectiveness of both resistance factors with higher pool level and various air injection rate.

3.3 Particle size distribution in axial direction

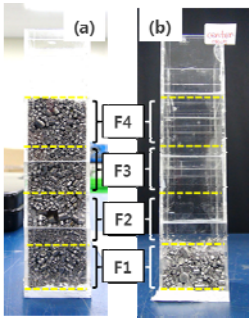

Fig. 10. Particle size distribution in axial direction of center region: (a) the QPC tests, (b) the TPC tests

To investigate the change of the particle size distribution in the axial direction, particle sampling was carried out for every 30 mm height of the particle sampling cups. Since there was concentrated particle sedimentation only at the center region in the QPC tests, the center region for both tests was investigated. Depending on the sedimentation quantity, four layers were sampled in the center region of the QPC tests, however, only one layer was possible with the TPC tests due to the small amount of sedimentation (see **Fig. 10**).

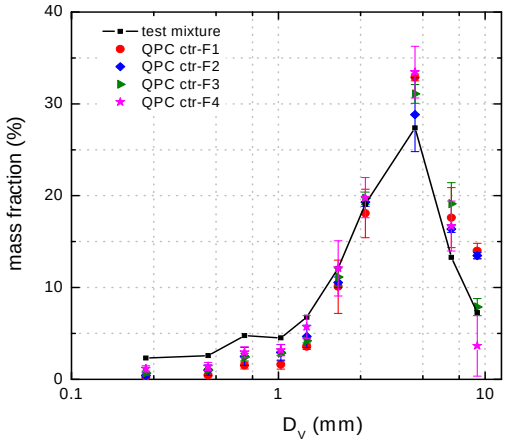

Fig. 11. Particle size distribution of the center region in axial direction of the QPC tests

Figure 11 shows the particle size distribution of the center region of the QPC tests. The lowest layer, QPC ctr-F1, which experienced the biggest resistance at the particle mixture jet head, exhibited the least mass fraction for the particles of small diameters and high mass fraction for the particles of large diameters. The mass fractions of the small particles increase with the axial distance, however, clear differentiation in the overall range of particle sizes was not exhibited in the test conditions of this study.

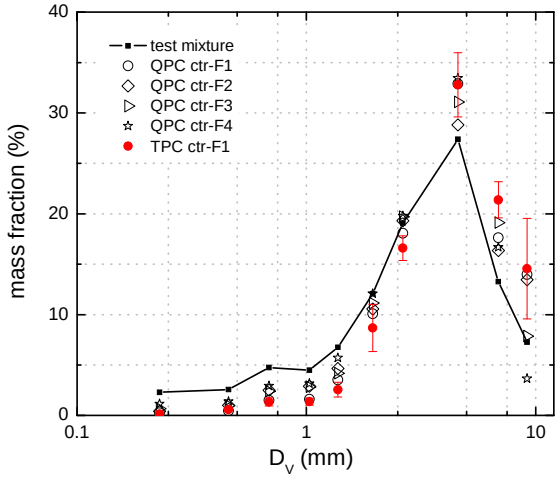

Fig. 12. Comparison of the particle size distribution for the center region in axial direction

We compared the particle size distribution of the center region for both conditions (see **Fig. 12**). The changes in the particle size distribution of the TPC tests were same as those of the QPC tests, and the degree of changes was higher. Additional tests with the particle mixture of larger volume are necessary to investigate the particle size distribution of more layers in the axial direction in TPC.

3.4 porosity

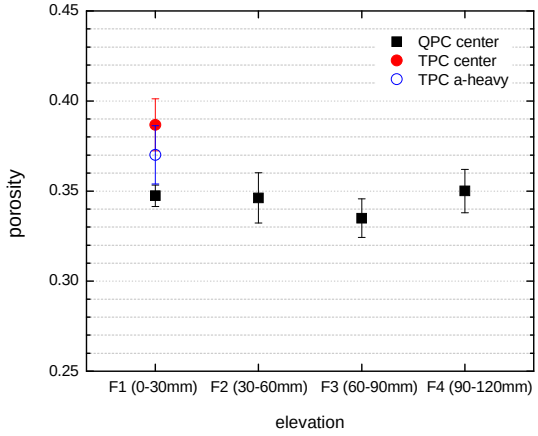

Fig. 13. Porosity of the center region in axial direction

Figure 13 shows the porosity of the both tests at the center region. The QPC tests showed almost constant porosity of around 0.34 along the elevation. The porosity of the TPC tests was about 0.39 and 0.37 for F1 level of the center and the heavy sedimentation side of the region a.

4. Conclusion

An experimental investigation was carried out for the internal structure of ex-vessel corium debris bed in the flooded cavity during sever accident. Moderate corium discharge in high flooding level was assumed for full fragmentation of melt jet. The test particle mixture was prepared by following an empirical correlation, which reflects the particle size distribution of various FCI tests. The vapor generation by decay heat of the corium debris bed on the bottom of the cavity was simulated using air injection. The local particle sedimentation quantity, particle size distribution change in radial direction and axial direction, and porosity was measured. In general, mass fractions of the small particles increased along the radial direction from the center, while mass fractions of the large particles decreased. Also, mass fractions of the small particles increased with the axial direction from the bottom, while mass fractions of the large particles decreased. In the QPC tests, the porosity in the axial direction from the bottom was almost constant, and the porosity of the TPC tests was slightly higher than that of the QPC tests.

ACKNOWLEDGEMENT

This work was sponsored by the Nuclear Safety Research Program of the Korea Radiation Safety Foundation grants funded by Korean government(NSSC) (Grant Code: 1305008-0113-HD140). And authors give thanks to Mr. Jun Hyun Kim at Mech. Eng. Dept., POSTECH for technical supports.

REFERENCES

[1] Yakush, S., Kudinov, P., and Dinh, T.-N., 2009, "Multiscale simulations of self-organization phenomena in the formation and coolability of corium debris bed," The 13rd International Topical Meeting on Nuclear Reactor Thermal Hydraulics (NURETH-13), Kanazawa City, Ishikawa Prefecture, Japan.

[2] Kim, E., Lee, M., and Park, H. S., 2014, "Development of Ex-Vessel Corium Debris Bed under Two-Phase Natural Convection Flows in Flooded Cavity Pool during Severe Accident," The Korean Nuclear Society Autumn Meeting, Korean Nuclear Society, Pyeongchang, Korea.

[3] Ma, W. M., and Dinh, T. N., 2010, "The effects of debris bed's prototypical characteristics on corium coolability in a LWR severe accident," Nucl Eng Des, 240(3), pp. 598-608.

[4] Thakre, S., Li, L., and Ma, W., 2014, "An experimental study on coolability of a particulate bed with radial stratification or triangular shape," Nucl Eng Des, 276, pp. 54-63.

[5] Magallon, D., 2006, "Characteristics of corium debris bed generated in large-scale fuel-coolant interaction experiments," Nucl Eng Des, 236(19), pp. 1998-2009.

[6] Moriyama, K., Maruyama, Y., Usami, T., and Nakamura, H., 2005, "Coarse break-up of a stream of oxide and steel melt in a water pool. Contract research," Japan Atomic Energy Research Inst., Kashiwa, Chiba (Japan).